Обзор ArXiv/astro-ph, 18-24 ноября 2021

От Сильченко О.К.

ArXiv: 2111.11627

The SAMI Galaxy Survey: the drivers of gas and stellar metallicity differences in galaxies.

A. Fraser-McKelvie[1,2⋆], L. Cortese[1,2], B. Groves[1,2], S. Brough[3,2], J. Bryant[4,5,2], B. Catinella[1,2], S. Croom[4,2], F. D'Eugenio[6,7], Á. R. López-Sánchez[8,9,2], J. van de Sande[4,2], S. Sweet[10,2], S. Vaughan[4], J. Bland-Hawthorn[4], J. Lawrence[8], N. Lorente[11], and M. Owers[9,12,2].

[1] *International Centre for Radio Astronomy Research, The University of Western Australia, 35 Stirling Hwy, 6009 Crawley, WA, Australia*
[2] *ARC Centre of Excellence for All Sky Astrophysics in 3 Dimensions (ASTRO 3D)*
[3] *School of Physics, University of New South Wales, NSW 2052, Australia*
[4] *Sydney Institute for Astronomy (SIfA), School of Physics, The University of Sydney, NSW 2006, Australia*
[5] *Australian Astronomical Optics, AAO-USydney, School of Physics, University of Sydney, NSW 2006, Australia*
[6] *Cavendish Laboratory and Kavli Institute for Cosmology, University of Cambridge, Madingley Rise, Cambridge, CB3 0HA, United Kingdo*
[7] *Sterrenkundig Observatorium, Universiteit Gent, Krijgslaan 281 S9, B-9000 Gent, Belgium*
[8] *Australian Astronomical Optics, Macquarie University, 105 Delhi Rd, North Ryde, NSW 2113, Australia*
[9] *Department of Physics and Astronomy, Macquarie University, NSW 2109, Australia*
[10] *School of Mathematics and Physics, University of Queensland, Brisbane, QLD 4072, Australia*
[11] *AAO-MQ, Faculty of Science & Engineering, Macquarie University. 105 Delhi Rd, North Ryde, NSW 2113, Australia*
[12] *Astronomy, Astrophysics and Astrophotonics Research Centre, Macquarie University, Sydney, NSW 2109, Australia*

24 November 2021

ABSTRACT

The combination of gas-phase oxygen abundances and stellar metallicities can provide us with unique insights into the metal enrichment histories of galaxies. In this work, we compare the stellar and gas-phase metallicities measured within a $1R_e$ aperture for a representative sample of 472 star-forming galaxies extracted from the SAMI Galaxy Survey. We confirm that the stellar and interstellar medium (ISM) metallicities are strongly correlated, with scatter

Обзор SAMI

fused fibre hexabundles (Bland-Hawthorn et al. 2011; Bryant et al. 2014) with a high (75%) fill factor. Each bundle contained 61 fibres of 1.6″ diameter resulting in each integral field unit (IFU) having a diameter of 15″. The IFUs, as well as 26 sky fibres, were plugged into pre-drilled plates using magnetic connectors. SAMI fibres were fed to the double-beam AAOmega spectrograph (Sharp et al. 2015), which allowed a range of different resolutions and wavelength ranges. The SAMI Galaxy survey employed the 580V grating between 3750–5750 Å giving a resolution of R=1810 ($\sigma = 70.4$ km s^{-1}) at 4800 Å and the 1000R grating from 6300–7400 Å giving a resolution of R=4260 ($\sigma = 29.6$ km s^{-1}) at 6850 Å (Scott et al. 2018). 83% of galaxies in the SAMI target catalogue had coverage out to 1 effective radius ($1R_e$, Bryant et al. 2015).

The SAMI Galaxy Survey was comprised of a sample drawn from the Galaxy and Mass Assembly (GAMA; Driver et al. 2011) survey equatorial regions (Bryant et al. 2015), and an additional sample of eight clusters (Owers et al. 2017). SAMI Data Release 3 (DR3; Croom et al. 2021) contains observations of 3068 galaxies and is the final data release of the SAMI survey. SAMI DR3 includes observations spanning $0.04 < z < 0.128$ and $7.42 < \log M_\star[\mathrm{M}_\odot] < 11.89$ (corresponding to an r-band magnitude range of $18.4 < m_r < 12.1$), with environments ranging from underdense field regions to extremely overdense clusters.

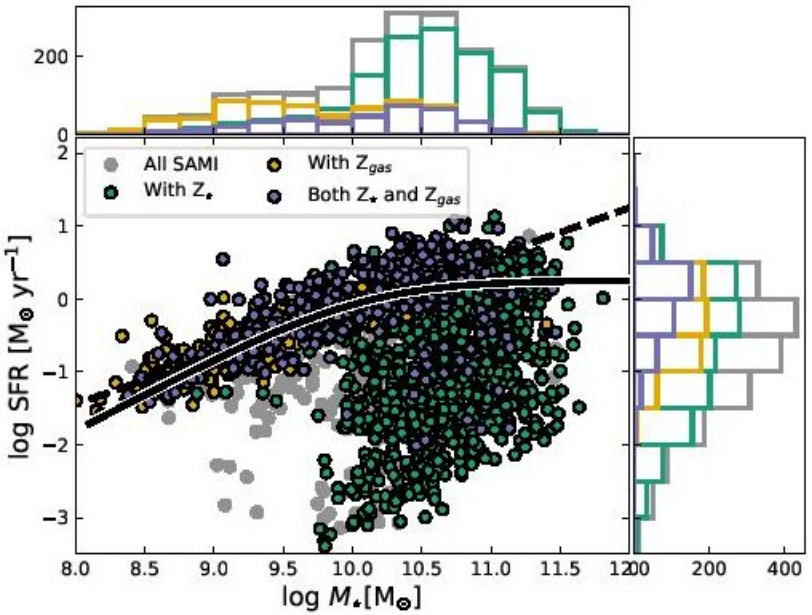

Figure 1. The SAMI galaxies used in this work in the SFR-stellar mass plane. Histograms in mass and SFR for each population are shown to the top and right side of the plot, respectively. Purple points are 472 galaxies with Z_{gas} and $Z_\star$ information, satisfy the S/N cuts discussed in the text and are the sample used in the following analysis. Orange points have only Z_{gas}, green points have only $Z_\star$, and grey points have neither indicator. The curved and linear star-forming main sequence lines of Fraser-McKelvie et al. (2021) are shown in black for reference.

Определение звездной металличности: SFH от pPXF

We employed the MILES SSP model templates (Vazdekis et al. 2010) with ages 0.08, 0.10, 0.13, 0.16, 0.20, 0.25, 0.32, 0.40, 0.50, 0.63, 0.79, 1.0, 1.26, 1.58, 2.0, 2.51, 3.16, 3.98, 5.01, 6.31, 7.94, 10.0, 12.59, 15.85 Gyr , metallicities -1.71, -1.31, -0.71, -0.4, 0.0, 0.22 , and 'baseFe' (Milky Way value) α enhancement.

Previous work has shown that full spectrum fitting often struggles to fit an excess of blue light within a galaxy (e.g. Cid Fernandes & González Delgado 2010) normally attributed to horizontal branch stars in the planetary nebula phase (e.g. Yi 2008). As noted in Peterken et al. (2020), this light is not accounted for in old SSP template spectra, and so full spectral fitting software often attributes it to young, metal-poor populations. For our stellar population age and metallicity estimates, we therefore follow the method of Peterken et al. (2020) and whilst we use the entire template range in our fits, we remove the contribution of the youngest SSP templates (in our case 0.08 Gyr) weights when calculating average ages and metallicities. Peterken et al. (2020) show that older stellar populations are unaffected by the method by which the younger populations are modelled, and so are robust.

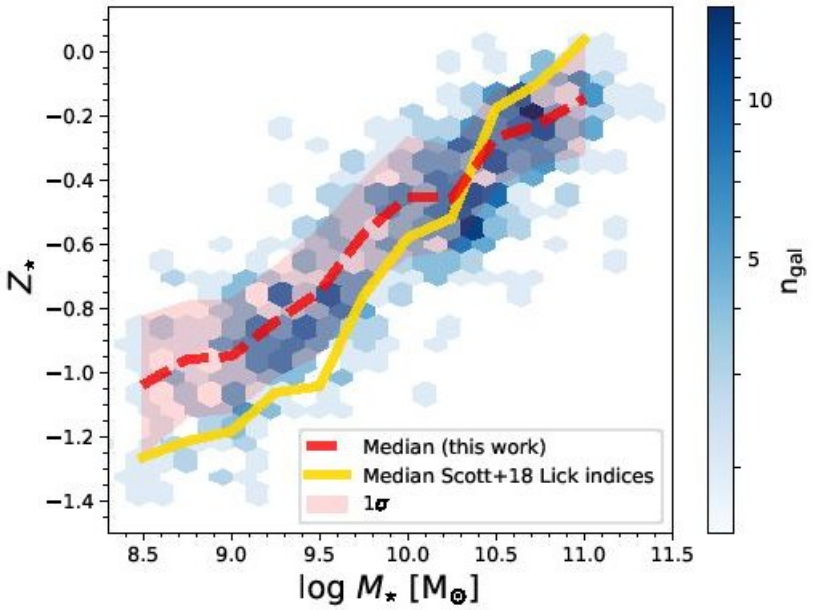

Figure 2. Stellar mass-stellar metallicity relation ($M_\star - Z_\star$ relation) derived via light-weighted stellar population analysis using the full spectral fitting code pPXF. The mass-metallicity relation is apparent, with the median of the relation shown as a dashed red line and the shaded region is the 1σ scatter. The average scatter in the $M_\star - Z_\star$ relation is 0.15 dex. For comparison, the median $M_\star - Z_\star$ relation for the same SAMI galaxies using the Lick index-derived stellar metallicities presented in Scott et al. (2018) is shown in gold.

Определение газовой металличности

The R-calibration of Pilyugin & Grebel (2016) was employed to determine oxygen abundances, as replicated below:

$$(\mathrm{O/H})^{*}_{\mathrm{R,U}} = 8.589 + 0.022\ \log(R_3/R_2) + 0.399\ \log N_2 + (-0.137 + 0.164 \log(R_3/R_2) + 0.589 \log N_2) \times \log R_2, \quad (1)$$

when $\log N_2 \geqslant -0.6$

$$(\mathrm{O/H})^{*}_{\mathrm{R,L}} = 7.932 + 0.944\ \log(R_3/R_2) + 0.695 \log N_2 + (0.970 - 0.291 \log(R_3/R_2) - 0.019 \log N_2) \times \log R_2, \quad (2)$$

when $\log N_2 < -0.6$, and where:
$R_2 = I_{[\mathrm{OII}]\lambda3727+\lambda3729}/I_{\mathrm{H}\beta}$,
$R_3 = I_{[\mathrm{OIII}]\lambda4959+\lambda5007}/I_{\mathrm{H}\beta}$,
$N_2 = I_{[\mathrm{NII}]\lambda6548+\lambda6584}/I_{\mathrm{H}\beta}$,
and $(\mathrm{O/H})^{*}_{\mathrm{R,U}}$ and $(\mathrm{O/H})^{*}_{\mathrm{R,L}}$ refer to the upper and lower tracks of the relation respectively, and $(\mathrm{O/H})^{*}_{\mathrm{R}} \equiv 12 + \log(\mathrm{O/H})_{\mathrm{R}}$.

We define $Z_{gas} \equiv 12 + \log(\mathrm{O/H})_{\mathrm{R}} - 8.76$, or $Z_{gas} \equiv \log(\mathrm{O/H}) + 3.24$, where the solar value oxygen abundance of 8.76 (Nieva & Przybilla 2012) has been subtracted. The

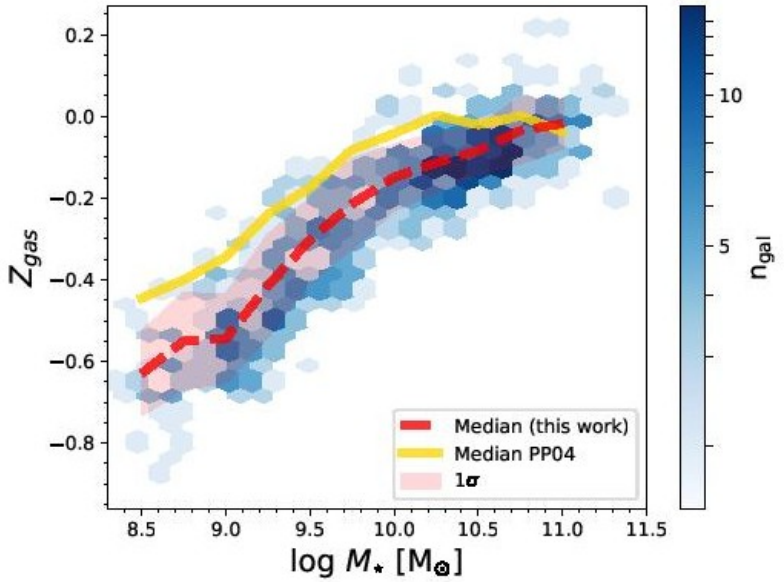

Figure 3. The $M_\star - Z_{gas}$ relation for SAMI galaxies in this work derived using the empirical calibration of Pilyugin & Grebel (2016). Hexbins are coloured by the number of galaxies in each bin. The red dashed line denotes the median of this relation, and the red shaded region the 1σ scatter, the average of which is 0.08 dex. For comparison, the median derived from the empirical O3N2-based calibration of Pettini & Pagel (2004) is shown in gold. The flattening of the $M_\star - Z_{gas}$ relation at high Z_{gas} as seen in previous works is apparent.

Их сравнение

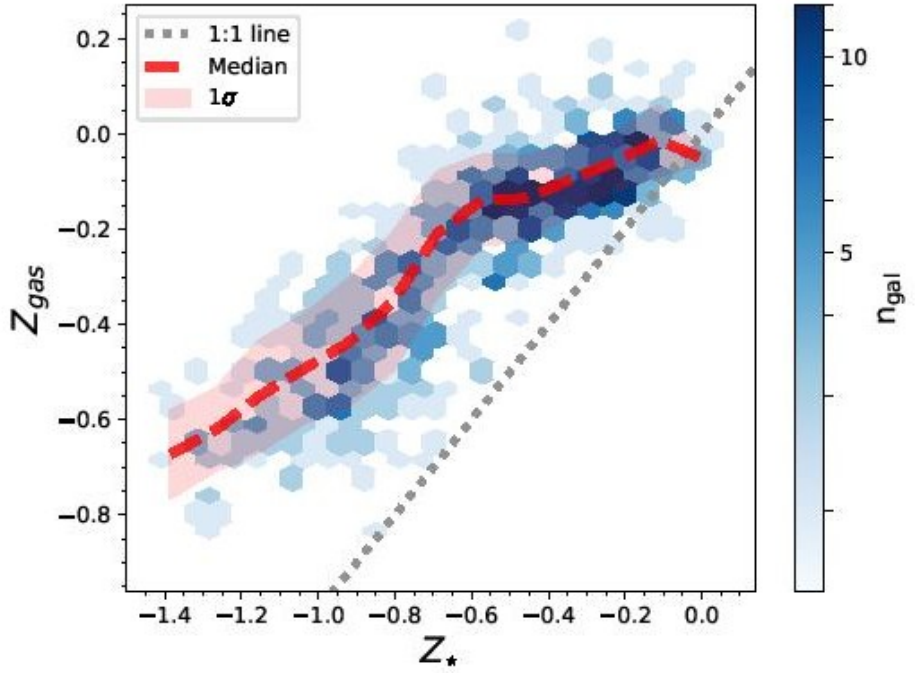

Figure 4. Comparison of Z_{gas} using the Pilyugin & Grebel (2016) calibration to the pPXF-derived light-weighted $Z_\star$ for SAMI galaxies. Hexbins are coloured by the number of galaxies in each bin. The red dashed line denotes the running median and the shaded region is the 1σ scatter. For all but the most stellar metal-rich galaxies, $Z_\star$ is always lower than Z_{gas}.

От чего зависит разница?

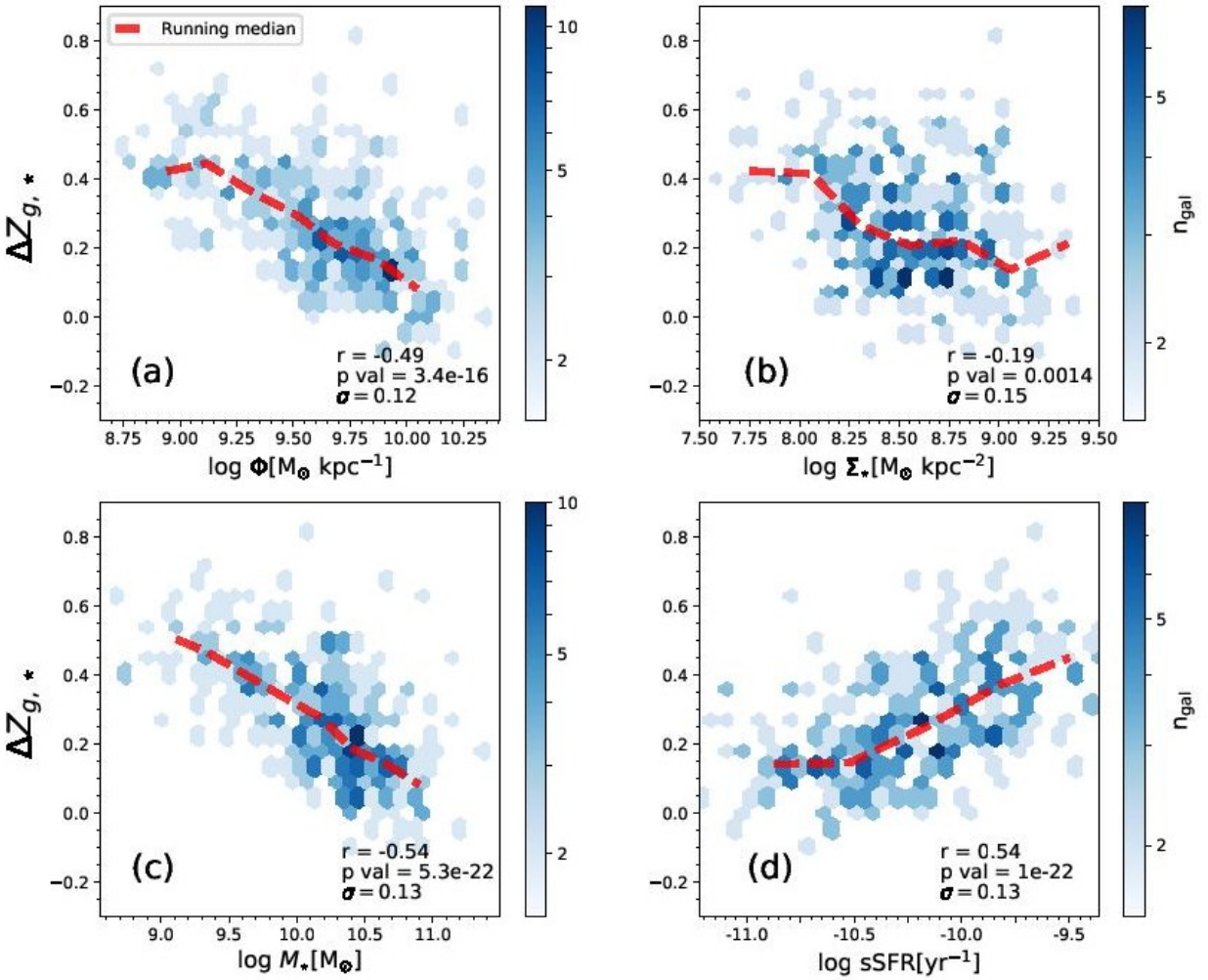

The correlation between $\Delta Z_{g,\star}$ and four galaxy properties that correlate with Z_{gas} and $Z_\star$ individually. For ea
correlation coefficient (r), p-value, and the vertical scatter in the correlation (σ) are shown. The red dashed lin

Два загадочных графика

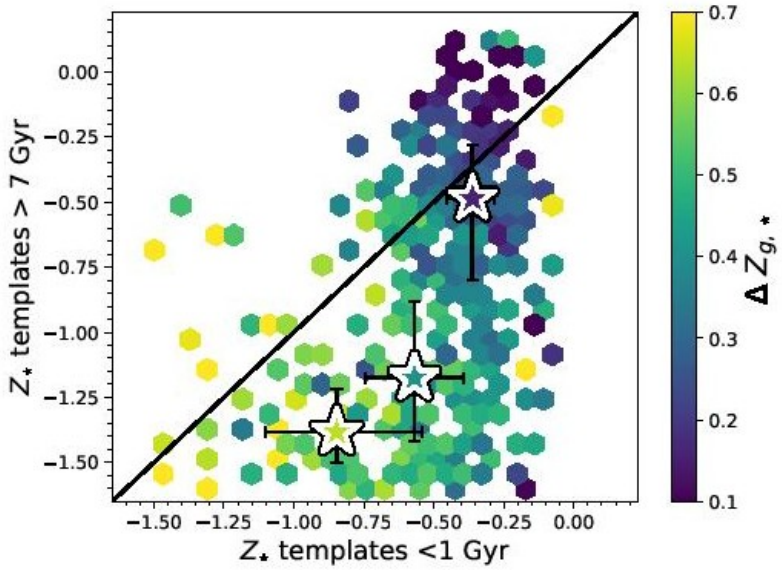

Figure 7. Splitting the full spectral fit results into young (< 1 Gyr) and old (> 7 Gyr) stellar populations. The stellar metallicity $Z_\star$ of the < 1 Gyr vs. > 7 Gyr stars within the same galaxy are plotted. Points are coloured by their metallicity ratio $\Delta Z_{g,\star}$, with the large star-shaped markers representing median values in three bins of $\Delta Z_{g,\star}$. Only galaxies with > 10% of light in both young and old templates are plotted. The majority of < 1 Gyr stars are metal rich, but the metallicity of the > 7 Gyr stars is correlated with the metallicity ratio.

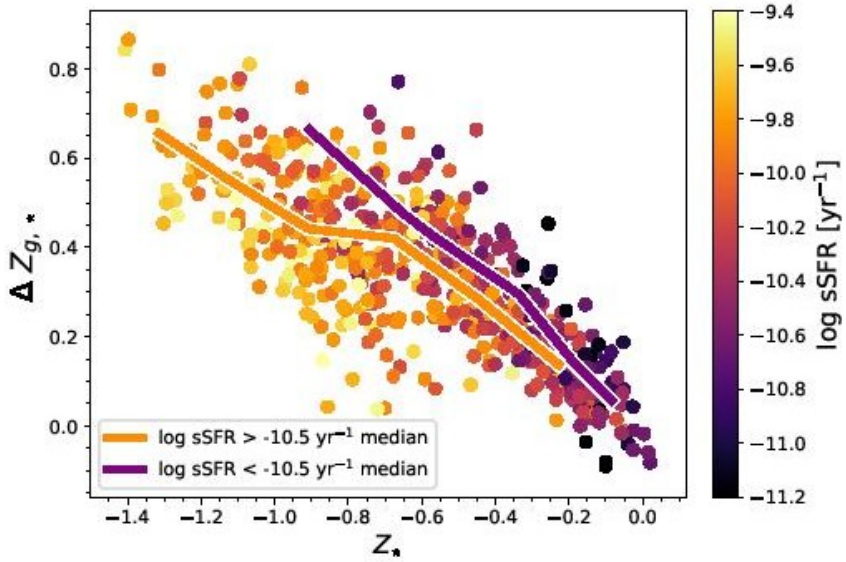

Figure 8. The variation of the metallicity ratio $\Delta Z_{g,\star}$ as a function of stellar metallicity indicator $Z_\star$. Points are coloured by the sSFR of the galaxy. The medians of two bins in sSFR are shown and diverge at low $Z_\star$. For a given $Z\star$, $\Delta Z_{g,\star}$ depends on the sSFR of the galaxy.

Вспомнили, что Z газа и звезд – это разные элементы; поправили почему-то только газ

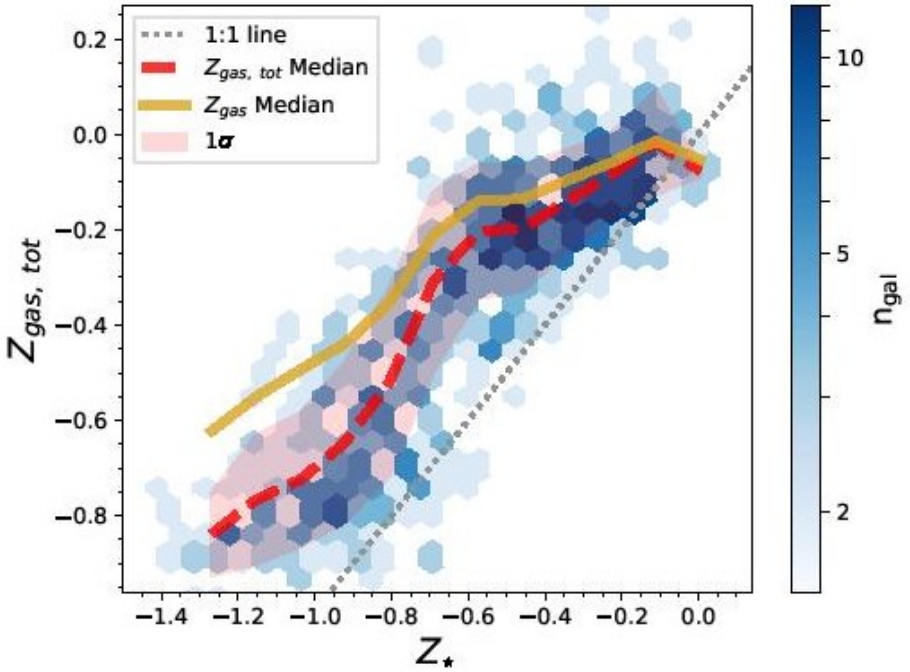

Figure 9. Comparison of the stellar and total gas metallicity indicators for SAMI galaxies. Hexbins are coloured by the number of galaxies in each bin. The red dashed line denotes the running median. The gold line denotes the median for Z_{gas} from Figure 4. While $Z_{gas,tot}$ and $Z_\star$ are more similar to one another than Z_{gas} and $Z_\star$ (especially at low metallicities), the stars are still almost always more metal-poor than the gas in the SAMI galaxies.

Но стало лучше: ближе к closed-box (но не для тех галактик…)

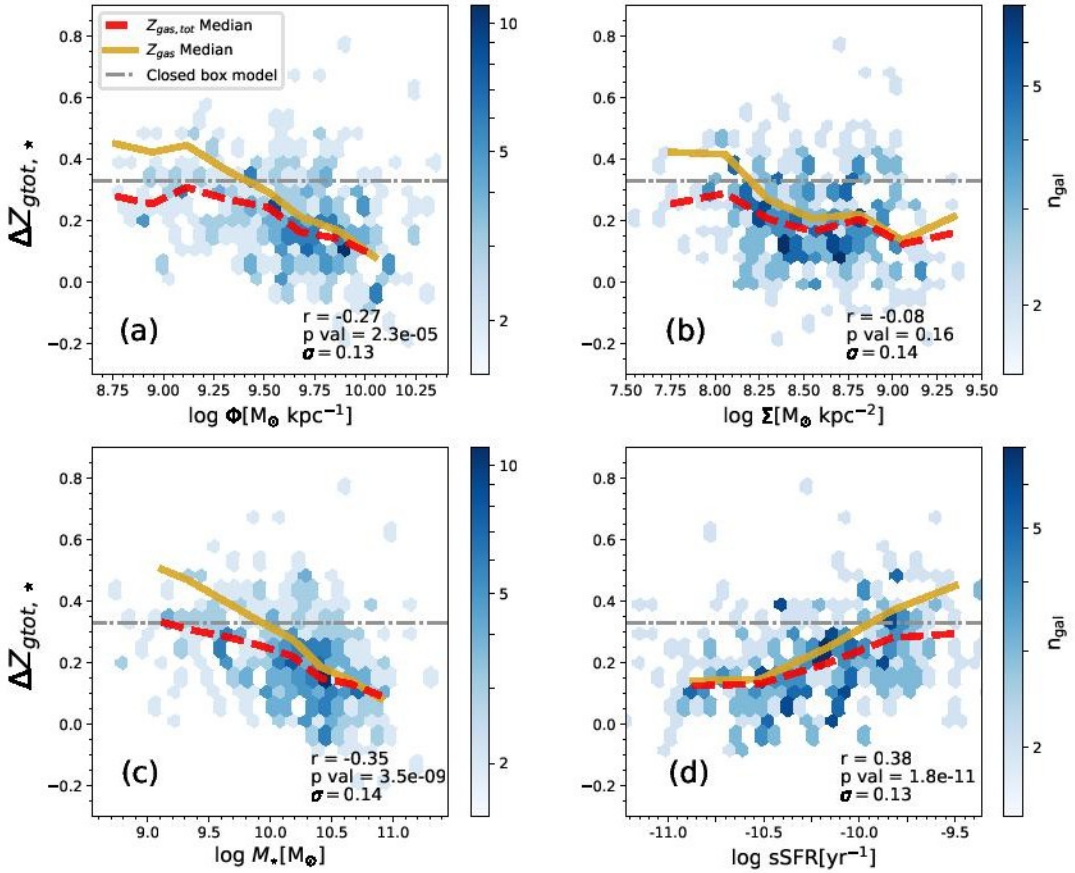

Trends in $\Delta Z_{gtot,\star}$ as a function of four galaxy properties. The red dashed line is the median of the SAMI gal
ows the median from Figure 5. The trends all flatten when using $Z_{gas,tot}$ instead of Z_{gas}, a reminder that g

А не поразводить ли нам руками?

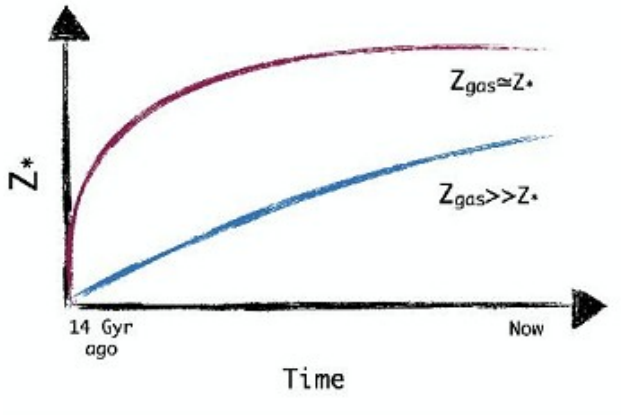

(a)

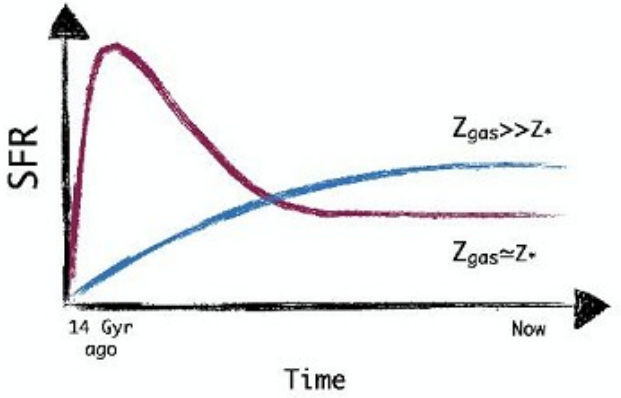

(b)

Figure 11. A cartoon representation of possible chemical evolution and star formation histories for two galaxies. The red line represents a galaxy with $\Delta Z_{g,\star} \sim 1$ that enriched early with an early burst of star formation. The blue line represents a galaxy where $\Delta Z_{g,\star} << 1$ at $z = 0$ and had a more sustained metal enrichment with low-level star formation. Panel (a) shows two possible metal enrichment pathways, and (b) the corresponding SFHs.